

Proceedings Article

Distal Fibula Fracture Treatment with Intramedullary Implant: Concept Assessment and Initial Verification

Elena Reznikova ^{a,*} · Nils Zander^b · Andreas Heede^b · Robert Wendlandt^{c,*}

^aStudent of Biomedical Engineering, Technische Hochschule Lübeck and Universität zu Lübeck, Lübeck, Germany

^bResearch and Development, Stryker Trauma GmbH, Schönkirchen, Germany

^cBiomechanics Laboratory, Clinic for Orthopedic and Trauma Surgery, University Medical Center Schleswig-Holstein, Lübeck, Germany

*Corresponding author, email: elena.reznikova@stud.th-luebeck.de, robert.wendlandt@uksh.de

Received 05 February 2025; Accepted 06 June 2025; Published online 18 July 2025

© 2025 Elena Reznikova *et al.*; licensee Infinite Science Publishing

This is an Open Access article distributed under the terms of the Creative Commons Attribution License (<http://creativecommons.org/licenses/by/4.0>), which permits unrestricted use, distribution, and reproduction in any medium, provided the original work is properly cited.

Abstract

This study examined the biomechanical performance of intramedullary nail implants for distal fibula fractures, particularly Weber B fractures. Simplified three-dimensional models were created to simulate the biomechanics of the leg during standing. Simulations were conducted with an axial load of 70 Newtons, with the fibula bearing 20 % of the total load from the body weight shared evenly between both legs. The results demonstrated that the intramedullary nail exhibited significantly lower stress levels compared to the traditional plate and screw construct. Peak Von Mises stress levels were 26 MPa in the nail's syndesmotic screw and 146 MPa at the screw-to-plate interface within the plate construct. These findings provide a rationale for the hypothesis that patients may be able to bear weight earlier after surgery.

1. Introduction

Ankle fractures are among the most common injuries in adults. The most frequently encountered fracture type in all age groups is a fracture of the lateral malleolus - the prominent distal head of the fibula on the outer side of the ankle [1]. The most prevail fracture type of the lateral malleolus is Weber B according to Weber classification [2].

This type of injury is often associated with dislocations, torn ligaments or syndesmosis damage that destabilize the ankle joint and require surgical treatment. [3] (see Figure 1). The current options for the ankle fracture fixation include open reduction and internal fixation (ORIF) with plate and screws as well as a minimally invasive intramedullary nail (IMN) (see Figure 2). The ORIF and IMN fixation methods typically restore the Weber-B

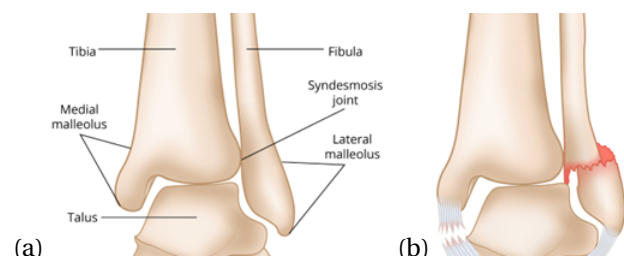


Figure 1: (a) Ankle anatomy overview (b) Lateral malleolus Weber B fracture and torn ligaments schematics.

fractured fibula through the screws in distal and proximal fibula as well as syndesmosis screw(s) in the tibia in case of the torn ligaments. The IMN, which is inserted into the intramedullary canal of the bone is a viable op-

tion for the treatment of the malleolus fractures providing significantly lower soft tissue compromise and low complication rate compared to the plate fixation. The typically smaller incisions decreases the risk of infection and further associated complications such as dehiscence or re-operation [4]. The nail treatment option also seems to enable early weight-bearing activities postoperatively [5].

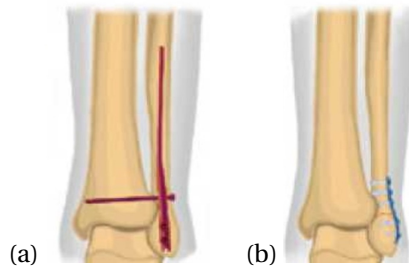


Figure 2: (a) Fixation with intramedullary nail and syndesmotic screw (b) Fixation with plate and locking screws.

These potential clinical advantages have to date limited biomechanical data supporting the difference in the mechanical performance of these two treatment methods.

This study aims to develop a simplified numerical test setup to assess and verify an intramedullary nail within the fibula under biomechanical stress, comparing it with the simplified plate fixation model under identical load conditions and interlocking configuration.

The results may provide an insight into the biomechanical performance of the nail and the plate fixation methods, serving as a foundation for further verification studies and intramedullary nail design input.

II. Methods and Materials

A systematic literature search was performed on the Database PubMed and throughout internal company resources from the Stryker Orthopaedic Modeling and Analytics (SOMA) database. The simplified 3D models and assemblies were created in Creo Parametric 3D Modeling Software (v. 10.0) with the reference to anatomical 3D models from SOMA. Simulations were performed in Creo Structural Analysis within Creo Parametric (v. 10.0).

II.I. Literature Review

The literature search was based on the anatomical structure and biomechanics of the ankle, in particular focusing on the fibula role and the implants common fixation methods for fractures. Insights from this review were considered for the design of the simplified construct assemblies and guided the selection of simulation parameters.

II.II. 3D Models and Assembly

The median standing foot model from SOMA served as a reference for the design of the simplified assembly and the implant construct alignment. The 3D models accounted key anatomical artifacts like tibia's plafond plane, apex of the syndesmotic joint, most common fracture pattern and the center axis of the bones.

In the simplified assembly, the fibula was represented as a cortical cylinder with a thickness of 3 mm and an outer diameter of 12 mm. The Weber B fracture cut was increased to a 4 mm gap to accentuate the fracture effect and create the worst-case scenario. The nail construct assembly included the uniform rod of 6 mm in diameter and 110 mm long as a nail. It was positioned into the fibula cylinder 5 mm above the fibula end plane. Distal and syndesmotic screws were appropriately inserted based on their anatomical positioning in a clinical scenario. The syndesmotic screw served as the proximal fixation for the fibula eliminating the need for additional fixation. The diameters of selected screws were 2.7 and 3.5 mm, respectively.

A separate plate fixation construct was also modeled, using the screws of the same lengths, diameters, trajectories and positioning respecting the fracture gap. Two additional screws of 2.7 mm in diameter were included per bone segment, resulting in six screws in the plate assembly replicating the clinical fixation scenario. The simplified locking plate had an internal curvature of 6 mm to match the bone outline and was 2 mm thick.

II.III. Simulation Setup

The load case was developed based on the literature review with the focus on creation of the worst-case scenario when the soft tissues are not considered and the oblique fracture gap is increased. For the load simulation, a two-leg stance was considered with the weight evenly distributed between both legs. The load of 70 Newtons simulating the 20 % of the weight bearing of one leg was applied axially on the distal fibular plane similarly to the study by Huang et al.[6]. The proximal surface of the fibula was fixed in all degrees of freedom. The syndesmotic screw surface area corresponding to the tibial fixation was also fixed, helping to exclude the tibia from the simulation. Screws were bonded with the fibular cortices and had a frictionless contact interface with the nail. The screws in the locking plate construct were merged with the plate. The interfaces between the bone and the nail, as well as the bone and the plate, had a contact with a friction coefficient of 0.2 [7]. The assemblies and the boundary conditions for both constructs are shown on Figure 3.

The metal components of the assemblies were modeled with the titanium alloy Ti6Al4V properties and the properties of the cortical bone were assigned to the fibula.

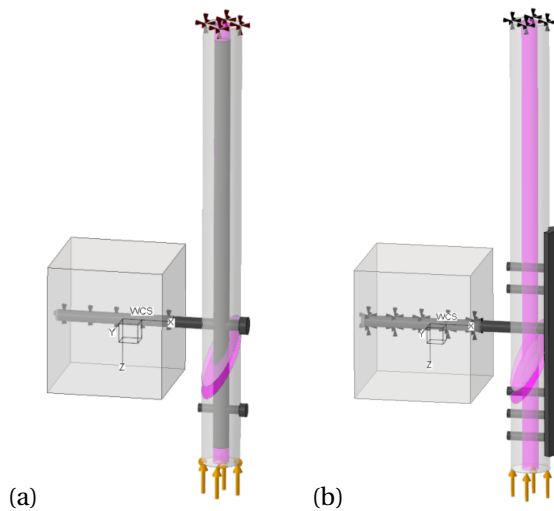


Figure 3: Simplified assembly with applied boundary conditions of (a) nail construct (b) plate construct. Rigid constraints are applied on proximal fibula and syndesmotic screws surfaces. Arrows represent direction and application area of the axial load.

The material properties used in this simulation are presented in Table 1.

Table 1: Assigned material properties [8], [9].

Material	Poisson's Ratio	Young's Modulus
Ti6Al4V	0.33	110.4 GPa
Cortical bone	0.3	17 GPa

After setting the constraints, applied load, and assigned materials, the meshes were automatically generated, resulting in 1381 elements and 489 nodes for the nail construct and 1320 elements and 570 nodes for the plate assembly. The setups further underwent static analysis.

III. Results and Discussion

III.I. Literature Review Outcome

Conducted literature research did not allow the establishment of the universally acceptable load case given the unique characteristics of human anatomy and movement [10]. It also revealed the limited biomechanical evidence comparing the strength and efficacy of nail and plate under the physiological load [4], [5]. Therefore, the setup and the load case required simplification of the simulation.

According to most relevant biomechanical studies on nails, the axial load ranging from 700 to 800 Newtons is applied to the ankle to mimic the single foot stance [5]. This value was also supported by the further studies

on ankle joint reaction forces [11]. The fibula typically carries around 20 % of the foot axial force [6], [12]. These findings defined the simplification features of the constructs designs, simulation setup and an axial load case.

To review the simulation results and establish their relevance, the simulation outcomes were compared with the ones from simulation study on the Weber B fibula fracture and the locking plate by Huang et al. [6].

III.II. Simulation Outcome

Upon simulations completion, the Von Mises Stress values were extracted and visualized. Figures 4 and 5 show the simulation results.

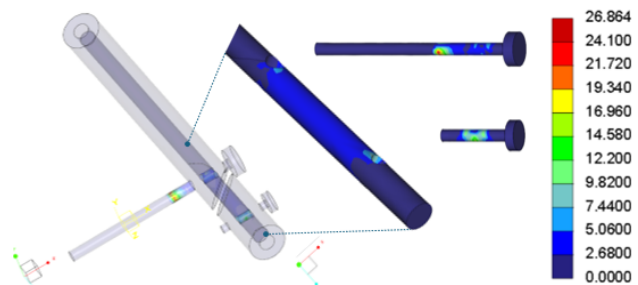


Figure 4: Von Mises Stresses results from simulation of the nail construct in MPa

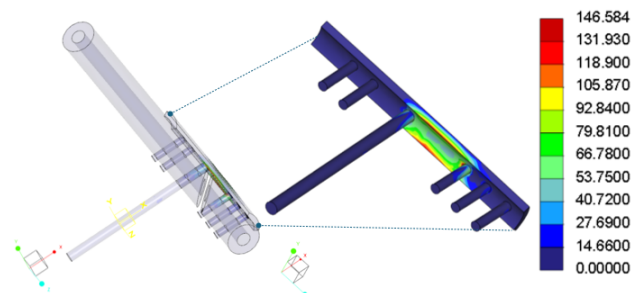


Figure 5: Von Mises Stresses results from simulation of the plate construct in MPa

The nail construct showed a maximum Von Mises Stress of 26.86 MPa mainly in the syndesmotic screw in the free area between fibula and tibia. The nail itself experienced the stresses below 16 MPa on the interfaces with the screw. The plate construct had the load peak of 146.58 MPa at the contact edges of the plate with syndesmotic and distal screws and the stress of 126 MPa along the fracture gap. These results indicate that the nail construct had significantly lower stresses under similar conditions, likely due to its central position within the bone canal, along with its thicker geometry in comparison to the plate.

The outcomes reported in the publication by Huang et al. [6] reflected the stress of 166.4 MPa in the plate.

As current study used a simplistic approach, it was unable to completely replicate the conditions and setup described in the aforementioned paper. Nevertheless, taking under the consideration the inherent inaccuracy of simulations due to approximation of the real-world conditions, these results can be regarded as comparable. This finding emphasizes the necessity to address the limitations of the study.

III.III. Limitations

The construct assemblies consisted of highly simplified anatomical representations, neglecting elements like ligaments, articulation surfaces and muscles that potentially influence the load distribution and stress outcomes. Additionally, the bone-to-implant interface was simplified considering the tight fit, uniform cortex thickness and the bone intramedullary canal geometry. The oblique axis of the fibula was ignored, and fixation points were minimized, which could have influenced load distribution across the construct. Notably, the syndesmotic screw's function as a compression link between fibula and tibia was not fully represented, as it was modeled and constrained in a locked state rather than actively allowing for compression.

IV. Conclusion

The findings of this study assess the concept of using an intramedullary implant for distal fibula fracture treatment. It showcases the biomechanical performance comparison of the locking plate and the nail constructs using highly simplified models with the consideration of limitations. The intramedullary nail construct showed significantly lower stress levels and improved load sharing capabilities under simulated weight bearing axial load. It is supporting the hypothesis of the earlier weight bearing possibility for patients with fibular fractures treated with the intramedullary nail.

The simulation results lend further credence to the continued development of the intramedullary implant. Additionally, the findings can contribute to potential enhancement of the construct design through identification of the highest stress concentration areas. Further studies could explore multiple screw configurations and variable fixation trajectories to distribute stresses more effectively. Moreover, additional load case applications could be considered for better mimicking the physiological load and more detailed verification of the constructs.

Acknowledgments

The work has been carried out at Stryker Trauma GmbH within the Research and Development Department.

Research Funding: No external funding was involved.

Author's Statement

Conflict of interest: Authors state no conflict of interest. Informed consent: Not applicable, as this study did not involve human participants. Ethical approval: Not applicable, as the research did not involve human or animal subjects.

References

- [1] R. Elsoe, S. E. Ostgaard, *et al.* Population-based epidemiology of 9767 ankle fractures. *Foot and Ankle Surgery*, 22(1):34–39, 2016, doi:10.1016/j.fas.2016.11.002.
- [2] M. Hollensteiner, S. Sandriesser, H. Krauss, *et al.* Three internal fixation methods for danis-weber-b distal fibular fractures: A biomechanical comparison in an osteoporotic fibula model. *Foot and Ankle Surgery*, 28(7):845–851, 2022, doi:10.1016/j.fas.2021.11.006.
- [3] American Academy of Orthopaedic Surgeons, Ankle fractures (broken ankle), Online, Accessed: 2025-January-04, n.d. URL: <https://orthoinfo.aaos.org/en/diseases--conditions/ankle-fractures-broken-ankle/>.
- [4] A. K. Attia, A. Fayed, K. Mahmoud, *et al.* Locked intramedullary nailing provides superior functional outcomes and lower complication rates than plate fixation of distal fibula fractures. a systematic review and meta-analysis of comparative studies. *Foot and Ankle Surgery*, 28:986–994, (7) 2022, doi:10.1016/j.fas.2022.02.005.
- [5] F. C. Kohler, P. Schenk, *et al.* Fibula nail versus locking plate fixation—a biomechanical study. *Journal of Clinical Medicine*, 12(2):698, 2023, doi:10.3390/jcm12020698.
- [6] S. Huang, J. Zhu, H. Xing, *et al.* Finite element analysis and a pilot study of different fixation constructs for danis-weber a and b lateral malleolus fractures. *BMC Musculoskeletal Disorders*, 24:981, (1) 2023, doi:10.1186/s12891-023-07115-0.
- [7] U. Simon, P. Augat, A. Ignatius, *et al.* Influence of the stiffness of bone defect implants on the mechanical conditions at the interface—a finite element analysis with contact. *Journal of Biomechanics*, 36(8):1079–1086, 2003, doi:10.1016/S0021-9290(03)00114-3.
- [8] A. Alito, A. Vitali, A. Bruschetta, *et al.* Finite element analysis of the fibula's contribution to lower extremity torsional stiffness. *Journal of Orthopaedics*, 61:114–121, 2025, doi:10.1016/j.jor.2024.10.007.
- [9] Stryker Trauma GmbH, Internal report № A0051258, Rev AA, Internal company document, 2022.
- [10] M. Oosterwaal, S. Telfer, S. Tørholm, *et al.* Generation of subject-specific, dynamic, multisegment ankle and foot models to improve orthotic design: A feasibility study. *BMC Musculoskeletal Disorders*, 12:256, 2011, doi:10.1186/1471-2474-12-256.
- [11] F. Crenna, G. B. Rossi, and A. Palazzo, Ankle moment measurement in biomechanics, in *XXII World Congress of the International Measurement Confederation (IMEKO 2018)*, IOP Publishing, 1065, 182005, Genova, Italy: Journal of Physics: Conference Series, 2018, doi:10.1088/1742-6596/1065/18/182005.
- [12] Q. Wang, W. Michaeland, C. James, *et al.* Fibula and its ligaments in load transmission and ankle joint stability. *Clinical Orthopaedics and Related Research*, 330:261–270, 1996, doi:10.1097/00003086-199609000-00034.